International Journal of Microwave and Wireless Technologies

cambridge.org/mrf

Evolution of gain enhancement techniques in dielectric resonator antenna: applications and challenges

Ankita H. Harkare[1,2], Ashwin G. Kothari[3] and Ankit A. Bhurane[3]

[1]Department of Electronics and Communication Engineering, Shri Ramdeobaba College of Engineering and Management, Nagpur, India; [2]Department of Electronics and Communication Engineering, Indian Institute of Information Technology, Nagpur, India and [3]Department of Electronics and Communication Engineering, Visvesvaraya National Institute of Technology, Nagpur, India

Review Paper

Cite this article: Harkare AH, Kothari AG, Bhurane AA (2023). Evolution of gain enhancement techniques in dielectric resonator antenna: applications and challenges. *International Journal of Microwave and Wireless Technologies* **15**, 891–905. https://doi.org/10.1017/S1759078723000119

Received: 8 September 2022
Revised: 7 February 2023
Accepted: 7 February 2023

Keywords:
Dielectric resonator antenna (DRA); Gain Enhancement; Mode of Excitation; Stacked DRA; FSS Superstrate; EBG Structure; Hybrid DRA; DRA Array

Author for correspondence:
Ankita H. Harkare,
E-mail: ankitaharkare1187@gmail.com

Abstract

Dielectric resonator antennas (DRA) are advantageous due to their small size, high radiation efficiency, ease of excitation, and minimal metallic losses. Enhancing the gain of DRA will make them suitable for a variety of applications such as wireless communication technology. High-gain antennas are required for wireless communication to overcome the difficulties of high path loss. The researchers have presented numerous techniques, including stacked DRA, DRA array, and higher-order mode excitation for enhancing the gain. This article provides a comprehensive summary of the state of art techniques and geometries including stacking, frequency-selective surfaces superstrate, electromagnetic band gap structures, hybrid techniques, arrays, etc., for increasing DRA gain. Techniques to improve other parameters like bandwidth and radiation efficiency along with gain are also discussed. The challenges in each technique and the possible applications are presented. Based on the studies, it is observed that the DRA array technique is suitable for obtaining gains up to 19 dBi for radar-based applications. For low-profile DRA requirements, hybrid DRAs prove prolific in enhancing gain up to 16 dBi.

Introduction

For several decades, dielectric resonator antennas (DRA) are being studied and experimented with by many researchers and have found their way into several technologies which require a high level of antenna performance such as broadcast systems, geosynchronous earth orbit, satellite communications, navigation systems, and a large variety of radar systems. Although several existing metallic antennas like microstrip patch antennae can be utilized in such applications, at very high frequencies, and under hostile temperature conditions, these antennas undergo metallic losses [1]. There are two main enthralling reasons for the DRAs at mm-wave frequency spectrum replacing patch antennas with DRAs [2–4]. Firstly, the DRAs have higher antenna efficiency than patch antennas; antenna efficiency is not as important at low frequencies (microwave frequencies), but it is significant at mm-wave frequencies due to high propagation losses, necessitating high-performance transmitters and receivers. The fractional bandwidth is the second reason why DRAs are more appealing in mm-wave applications. It also has a small size, ease of excitation is lightweight, and low cost. The DRA consists of a dielectric substance that has low ohmic losses and uses a high dielectric constant material. This reduces dielectric and metallic losses resulting in high radiation efficiency, high integration, and increased impedance bandwidth [1]. A rectangular dielectric resonator antenna (RDRA) is easy to fabricate and has a greater degree of freedom [5]. The 3D DRA structure allows designers to have greater freedom while designing than the 2D and 1D structures (like monopole antennas and microstrip patch antennas) [6]. It can have different shapes like rectangular, cylindrical, hemispherical, triangular, and cross-shaped [2, 7, 8]. These features make DRA reliable at high frequencies such as millimeter waves for many wireless applications and a possible contender for 5G applications [9]. Despite such interesting features, the gain performance of the dielectric antenna can be further enhanced for long-range wireless communication systems. For instance, in an underground mine wireless communication, the propagation properties are marked by a high level of oxygen absorption and rain attenuation. In such cases, high-gain antennas are required to compensate for attenuation effects and loss [10]. With the enhanced gain, DRAs can prove fruitful in such situations as they provide high radiation efficiency due to negligible conductor losses.

DRA has a size proportional to $\lambda_0/\sqrt{\varepsilon_r}$ [1]. Here, λ_0 is the free-space wavelength, and ε_r is the dielectric constant of the dielectric resonator (DR). DRAs provide high radiation efficiency since they exhibit no inherent conductor loss due to their material properties. This property is useful for millimeter (mm) wave antennas, as metal fabrication has a high loss rate and hence

lower radiation efficiency. Transmission lines can be coupled with DRAs which makes them suitable for integration into different planar transmission lines. The fabrication process is achievable by varying the position of the DRA with respect to the line. By choosing the appropriate resonator parameters, the operating bandwidth of a DRA can be varied over a wide range. The dielectric parameter has the potential to vary the bandwidth of the lower-order modes of a DRA by a fraction of a percent to about 20% or more. It has also been successful to use multiple modes radiating identically in hybrid combinations. DRAs can be excited in different modes to produce different radiation characteristics. Slots can be introduced in the DRA structure to enhance the bandwidth due to changes in the effective dielectric constant of the resonator (Table 1).

This paper provides an overview of various gain enhancement techniques, underlying principles, comparisons, and various challenges in the design. Furthermore, filtering DRA (FDRA) is also discussed which involves DRA along with a filter. In addition to a comprehensive collection of gain enhancement methods, from the year 1983 to the latest ones; this paper shows outcomes and identifies the key research areas for future work. This will serve as a guide to the reader for further research work on DRA.

The key contributions of this survey are:

- A detailed survey, evolution, and analysis of various emerging gain enhancement techniques of DRA are presented.
- Realization aspects of recent gain enhancements techniques for different types of DRA along with their respective characteristics are discussed.
- A detailed comparison of gain enhancement techniques with respect to the key parameters of DRA including gain, bandwidth, resonant frequency, and so on is covered.
- Key takeaways and research challenges in respective approaches are also discussed.

Section "Gain enhancement techniques" discusses the gain enhancement techniques with comparison, section "Comparison of gain enhancement techniques" discusses the comparison of various techniques based on performance parameters, and section "Conclusions and future scope" provides the conclusion and future scope in terms of challenges and research directions. The paper focuses more on the mm-wave frequency band in the later part as it is still an unexplored frequency range and is a future for the 5G wireless communication domain.

Table 1. List of abbreviation

S.N	Abbreviation	Definition
1	ADRA	Anisotropic dielectric resonator antenna
2	AXDRA	An array of cross dielectric resonator antenna
3	CDRA	Cylindrical dielectric resonator antenna
4	DR	Dielectric resonator
5	DRA	Dielectric resonator antenna
6	EBG	Electromagnetic band gap
7	FDRA	Filtering dielectric resonator antenna
8	FSS	Frequency-selective surface
9	HDRA	Hemispherical dielectric resonator antenna
10	MIMO	Multiple input multiple output
11	MMW	Millimeter wave
12	PCB	Printed circuit board
13	RDRA	Rectangular dielectric resonator antenna
14	SIG	Silicon image guide
15	SLLs	Side lobe levels
16	SMSH	Surface mounted short horn
17	SRDR	Stacked rectangular dielectric resonator
18	UWB	Ultra-wide band

Gain enhancement techniques

Due to the challenges and expectations of the continuously rising traffic explosion, substantial research and development are being done on fifth-generation (5G) wireless communication technology. The most effective strategy to fulfill the needs of the 5G communication system is to increase bandwidth. Switching to a higher-frequency band is necessary to handle the high data rate needed, which is in the gigabits per second range (Gbps) [11]. The fundamental issue with a higher-frequency band, however, is the substantial path loss in short-range communication by the short wavelengths. To overcome the difficulties of high path loss and increase the high-frequency transmission range, high-gain antennas are required [12]. Hence, to use DRAs as a possible replacement for traditional antennas, it is important to discuss their gain enhancement. A circularly periodic electromagnetic band gap (EBG) substrate can be used to enhance the gain of the antenna as reported by Denidni *et al.* [13]. Most techniques aim at reducing side lobe levels thereby increasing gain. High gain hybrid DRA with surface-mounted horn proposed by Elboushi *et al.* [14] is one such method. Various other techniques were researched [15–20] which resulted in gain enhancement as well. Using uniaxial anisotropic dielectric material inside the DR, the gain was increased as suggested by Fakhte *et al.* [21]. The experimental study on stacked DRA as proposed by Petosa and Thirakoune [22] can be used where two dielectric cylinders are stacked with an air gap between them. Such studies guide RF front-end designers to design antennae of the required configuration. Figure 1 shows the broad categories of gain enhancement techniques.

Stacked DRA

Stacking the different dielectric layers in the DRA is one of the promising gain enhancement techniques mentioned in [23–25]. Pan *et al.* [23] investigated a wideband, high-gain DRA. The antenna was made up of two dielectric layers with different permittivity and excited by a rectangular slot in the middle as depicted in Fig. 2(a). It has a bottom rectangular dielectric layer with low permittivity and a dielectric constant of 2.2 and a top rectangular dielectric layer with high permittivity and a dielectric constant of 15. The sides of the two layers are of the same length L, with different heights $h1$ and $h2$. The dimensions are set so that $L > h1 + h2$. This provides a low profile at the resonant frequency as explained by Essel *et al.* [24] and Mongia *et al.* [25]. The height variation causes the DRA to resonate in higher-order mode, thus improving the gain and radiation efficiency. A microstrip-coupled slot built on a substrate with a permittivity of ϵ_r feeds the antenna at its center. The top ground plane is created with a rectangular

https://doi.org/10.1017/S1759078723000119 Published online by Cambridge University Press

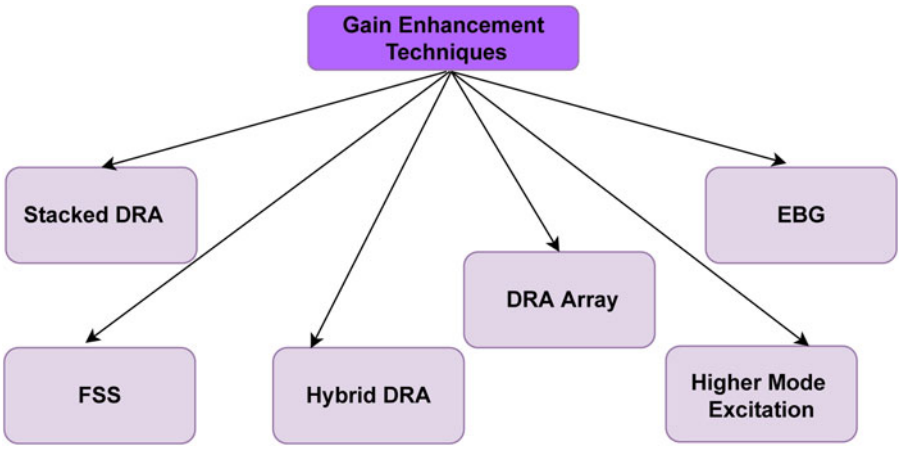

Fig. 1. A broad categorization of various gain enhancement techniques in DRA.

slot and a 50 Ω microstrip feedline. A stub of length l_m is etched on the other side of the substrate, as illustrated in Fig. 2(a). The DRA is *x*-polarized because it uses a *y*-directed slot for excitation. The high permittivity layer has $\varepsilon_r = 15$ whereas the low permittivity layer has $\varepsilon_r = 2.2$. The two layers result in two resonant modes in the passband. The TE^y_{111} mode at lower (4.35 GHz) frequencies causes the first resonance, whereas the TE^y_{131} mode at higher (5.4 GHz) frequencies causes the second. The TE^y_{121} mode cannot be excited because it requires a minimum *E*-field at the slot location. In the boresight direction ($\theta = 0°$), co-polarized fields are stronger than cross-polarized fields. The results confirm that the lateral and longitudinal resonances are responsible for the lower and upper modes, respectively. This means the two modes may be tuned independently, which is ideal for antenna construction. The work done by Pan *et al.* [23] was inspired by a double-layered high permittivity DR investigated by Hwang *et al.* [26] operating at a 1.8 GHz. The measured results show that the double-layered DR antenna achieved by stacking two layers of high permittivity ($\varepsilon_r = 38,\ 80$) has a 1.2 dB gain enhancement and 25% height reduction over a single-layered antenna. They also suggested that loss in radiation efficiency can be recovered by this introduction of a higher permittivity layer. The analysis provided by these two papers using stacking methodology provides an insight that by properly choosing the dielectric constants of the two layers as well as by changing the dimension ratios of height appropriately, wide impedance bandwidth up to 40% and an increase in gain up to 9 dBi is obtained. Similar stacking of uniaxial anisotropic material (UAM) with many layers inside a DR was proposed in [21, 27, 28]. Fakhte *et al.* [21] used a UAM inside the DR rectangular prism to improve the directivity of DRA functioning in the fundamental TE^y_{111} radiating mode. This is a unique technique for obtaining higher gain as compared to higher-order mode generation. The use of UAMs in RDRA improves the radiation from the side walls as compared to the top walls. This improves the boresight radiation pattern and hence the gain. Figure 2(b) shows the fabricated stacked DRA [21]. The permittivity tensor for a uniaxial anisotropic medium is given by equation (1).

$$\bar{\bar{\varepsilon}} = \begin{matrix} \varepsilon_x & 0 & 0 \\ 0 & \varepsilon_x & 0 \\ 0 & 0 & \varepsilon_z \end{matrix} \tag{1}$$

The concept of extraordinary and ordinary waves was explained in literature [29–31]. Lowering the value of ε_z in

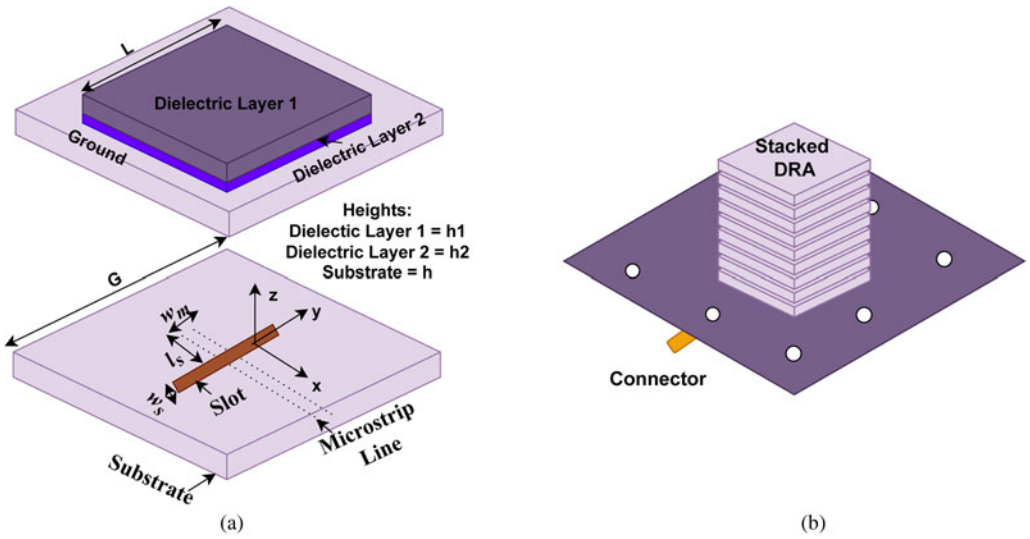

Fig. 2. (a) High gain stacked DRA with microstrip coupled slot. (b) An anisotropic stacked DRA.

https://doi.org/10.1017/S1759078723000119 Published online by Cambridge University Press

comparison to the value of ϵ_x significantly increases the electromagnetic (EM) field leakage from the sidewalls of ADRA as compared to the top wall. Anisotropic DRA's impedance bandwidth and gain are enhanced when ϵ_z is reduced, compared to isotropic DRAs. The drop in the effective dielectric constant of the structure is responsible for the anisotropic DRA's increased impedance bandwidth [32]. The directivity of rectangular DRA in the boresight direction is increased considerably. Similar anisotropic DRAs were explored by Yarga *et al.* in their research work suggesting better gain using hybrid and higher-order mode excitation [27, 28]. An interesting way of using the Yagi–Uda concept was introduced in DRA by Kishk [33] where different discs of the same dielectric material were connected through a nick-like structure of the same material. This reduced the cost as the material used was of the same dielectric constant and increased the directivity of the antenna. A two-, three-, and four-discs arrangement excited by the coaxial probe is shown in Fig. 3(a). The gain enhancement of 2.7 dBi for two discs and 3.6 dBi for three discs was obtained in [33]. The gain was found to be enhanced in stacked DRAs with respect to non-stacked DRAs. Another novel technique of improvisation was proposed by Xia *et al.* where a comb-like structure is placed above DRA to provide circular polarization [34]. However, the trapezoidal geometry of the DR along with the comb-like structure provides a stable radiation pattern in the boresight direction thereby increasing the gain up to 8.3 dBic. Stacking in trapezoidal geometry is shown in Fig. 3(b). Furthermore, Table 2 shows the performance comparison of some stacked DRA antennas. The graph of Fig. 4 shows briefly the increment in gain due to stacking. Despite all these advantages, stacked antennas do have limitations of being costly and bulky, and hence new techniques to enhance gain need to be explored.

Excitation of DRA in higher-order modes

Another important technique for gain enhancement in DRA is by exciting the DRA with higher-order modes. Higher-order modes were initially used to increase the impedance bandwidth of DRA [35–37]. The technique of using higher permittivity material for stacking was suggested for gain enhancement in the planar antenna of inverted *F* type by Hwang *et al.* [38] and the same concept is applied to DRA and the results are achieved. However, Petosa *et al.* investigated the use of higher-order mode excitation for gain enhancement using the FDTD simulation method [39]. A simple dielectric waveguide model for predicting radiation patterns was proposed by Petosa *et al.* where up to 5 dBi gain enhancement was obtained at higher-order modes as compared to the fundamental mode of excitation [22]. For a rectangular DRA having a dielectric constant of ε_r and dimensions of a, b, and d and with a perfect infinite ground plane, the resonant frequency of f_{mn} and $TE^{x}_{\delta mn}$ mode can be predicted using equations (2)–(4) given by Mongia *et al.* [40, 41].

$$k_x \tan\left(\frac{k_x}{2}\right) = \sqrt{(\varepsilon_r - 1)k_o^2 - k_x^2} \tag{2}$$

$$k_o = 2\pi f_o,\ k_y = \frac{m\pi}{b},\ k_z = \frac{n\pi}{d} \tag{3}$$

$$k_x^2 + k_y^2 + k_z^2 = \varepsilon_r k_o^2 \tag{4}$$

$$f_o = \frac{c}{2\pi\sqrt{\varepsilon_r}}\sqrt{k_x^2 + k_y^2 + k_z^2} \tag{5}$$

where k_x, k_y, and k_z are wavenumbers in x, y, and z directions respectively and k_o is free space wavenumber. The speed of light is represented by c. The value of wave numbers essentially depends on the mode of operation. When the antenna is functioning in its higher-order modes, the size and separation distance between the edges expand to several wave lengths [42]. As the electric field varies more quickly, the currents suffer a 180° phase shift in neighboring half cycles, which leads to high side lobe levels and distorted radiation patterns, while having high gain. Equation (6) [42] shows the relationship between gain (G) and effective aperture area and wavelength.

$$G = \frac{4\pi A_{eff}}{\lambda^2} \tag{6}$$

where A_{eff} is the effective aperture area and λ is the wavelength of the antenna. Therefore, exciting an antenna in a higher-order

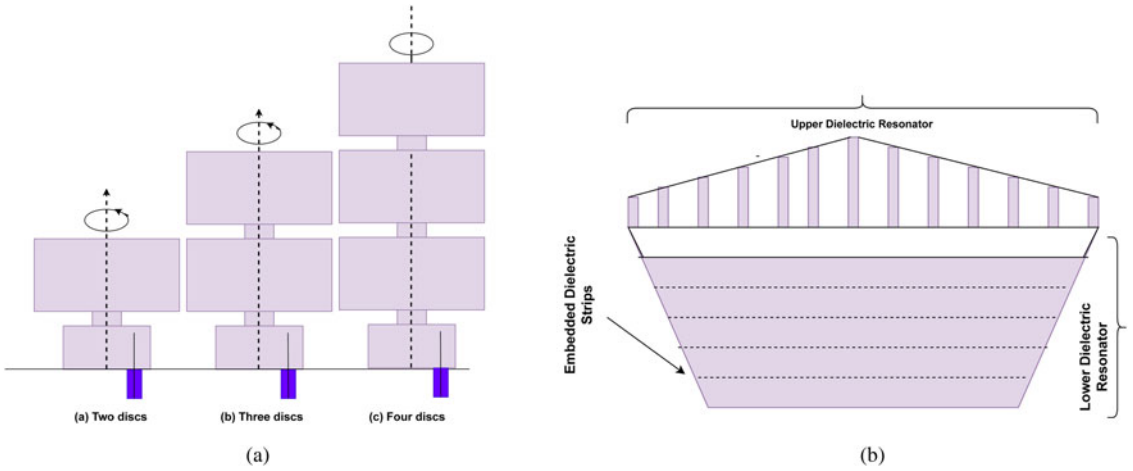

Fig. 3. (a) Stacked arrangement of DRA for enhanced gain. (b) Stacked trapezoidal comb-like DR for CP.

https://doi.org/10.1017/S1759078723000119 Published online by Cambridge University Press

Table 2. Performance comparison of stacked DRAs

Reference	No. of layers	Mode of excitation	Gain (dBi)	%BW
Hwang *et al.* (1997) [26]	2	–	6.2	2.7
Kishk (2005) (2 Discs) [33]	2	$HEM_{11\delta}$	7.8	20
Kishk (2005) (3 Discs) [33]	3	$HEM_{11\delta}$	8.7	16
Yarga *et al.* (2009) [27]	3	Hybrid TE^{y}_{101}, TM^{y}_{011}	6.51	1.62
Yarga *et al.* (2009) [28]	3	Higher-order mode	7.42	3.97
Pan *et al.* (2015) [23]	2	$TE_{\delta 15}$	9	40
Fakhte *et al.* (2016) [21]	2	Fundamental TE^{y}_{111}	8.4	20.6
Xia *et al.* (2022) [34]	2	$TE_{\delta 11}$ and $TE_{\delta 13}$	8.3	69.7

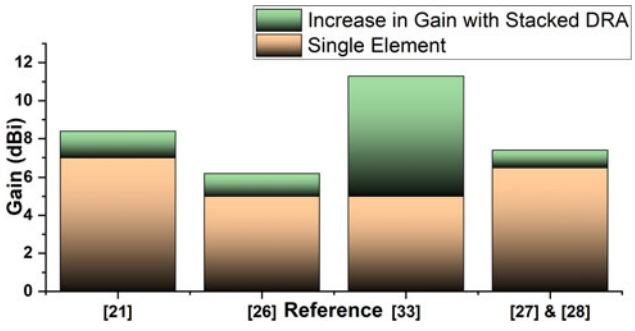

Fig. 4. Gain (dBi) increment using stacked arrangement of DRA.

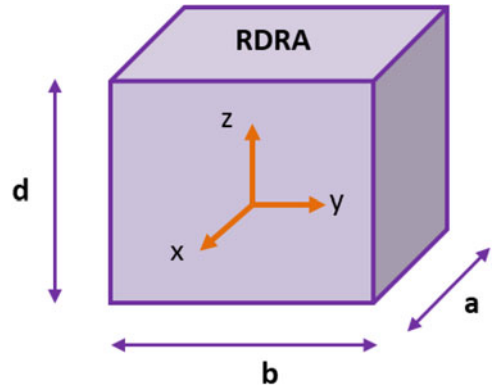

Fig. 5. RDRA with dimensions *a*, *b*, and *d*.

mode essentially increases the electrical area and hence the gain [16]. The dimensions of an RDRA considered by Mongia [41] are as per Fig. 5. Ali *et al.* [43] used a simple RDRA but excited it in $TE^{x}_{\delta 15}$ obtaining a high gain of 10.5 dBi. This was achieved by strategically using an aperture coupled feed line.

Higher-order excitation to receive a stable radiation pattern and improved gain was achieved by Liang *et al.* [44] by strategically developing an H-shaped DRA with a trapezoidal conformal feed. They selected a DR of a higher dielectric constant of 9.8 for improved bandwidth and better radiation patterns. A similar H-shape of the DRA was proposed by Fakhte *et al.* [45] by inserting grooves in the side wall of the DRA. The groove causes an increase in the magnitude of the electrical field, thus increasing the bore sight gain of the antenna to 9.6 dBi. Abdulmajid *et al.* [46] in their paper excited a hemispherical DRA (HDRA) in TE_{511} and TE_{711} by using a cross-slot feeding mechanism. Though the HDRA is multilayer, this methodology is used here for wider bandwidth and not for enhanced gain. This antenna is unique as it provides a gain of approximately 9.5 dBi in the mm-wave frequency range. Such high gain at mm-wave frequency is desirable for forthcoming 5G technology applications. The multilayer permittivities of 9, 4, and 3 for the inner, middle, and outer layers, respectively, were utilized. The gain is maintained by coating the DRA with two layers to provide a multistage transition and gives wide bandwidth. Hu *et al.* [47] proposed a FDRA using a microstrip-coupled slot from the bottom and open stub of the microstrip feedline. This FDRA was designed to provide two radiation nulls at band edges for filtering which was an extended work of the antenna proposed in [48]. In this paper [47], Hu *et al.* elaborated on the design with all four phases and proved the gain enhancement up to 4 dBi through separate slots in the feeding mechanism, thereby exciting the RDRA in higher mode. The development stages are shown in Fig. 6(i). It can be seen from Fig. 6(i–c), that the antenna III with slots in the coupled line causes the boresight gain to decrease significantly although the filtering functionality improved. Two parallel strips which improve the suppression in the upper stopband are introduced in antenna IV. This suppression helps improve the gain. Three resonant modes at 5, 5.7, and 6.07 GHz are obtained due to fundamental TE_{111}, TE_{311}, and hybrid Hybrid Electromagnetic (HEM) modes, respectively. Also, bending the DRA and exciting it with two sets of microstrip-coupled slots with an interval distance of a wavelength forms a 2×1 array, improving the gain to 9.05 dBi. Figure 6(ii) [47] shows this change in the configuration of antenna IV given in Fig. 6(i) [47].

Pan *et al.* [49] derived through their experimentations that when a slot for cross-coupling microstrip feed is placed at the center of the DRA, a TE_{pqr} mode can be excited only if *p*, *q*, and *r* all are odd numbers. For the odd-mode solution, the tangential electric field is antisymmetric about the middle plane which is an equivalent electric wall [50]. In [49], two DRAs were proposed to operate at TE_{115} and TE_{119} higher modes for mm-wave frequency of 24 GHz with a gain of 5.8 and 6.3 dBi for respective modes. The characteristic equations of the wavenumbers and for the TE_{pqr} mode were derived using Marcatili's approximation technique as mentioned by Mongia *et al.* [40, 41]. The isolation of modes can be obtained by carefully selecting DRA dimensions. A reconfigurable CP antenna was proposed in [51] with wideband and better gain. By removing a concentric annular column from its interior, the DRA element allows unidirectional HEM_{110}

https://doi.org/10.1017/S1759078723000119 Published online by Cambridge University Press

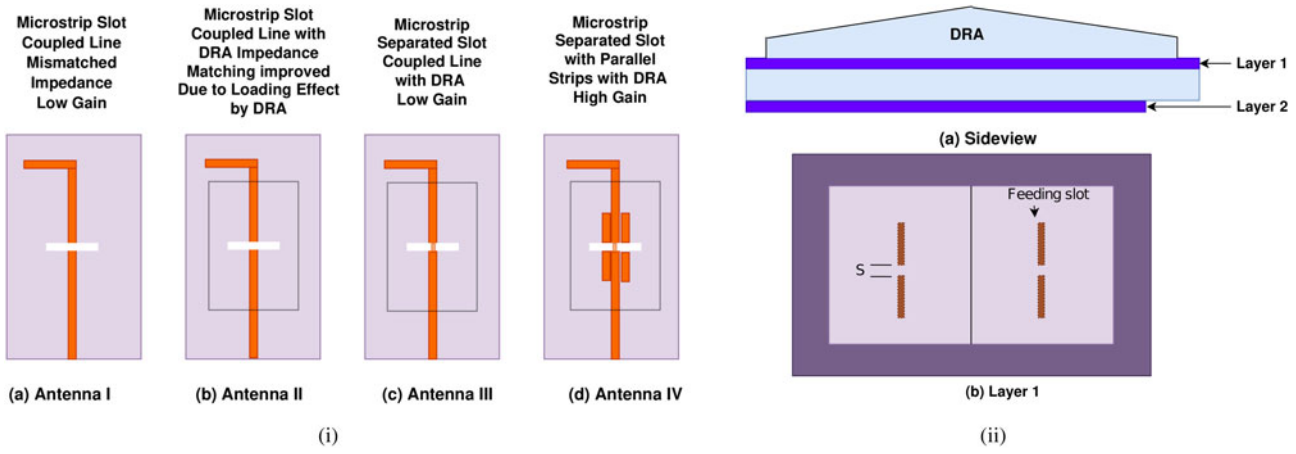

Fig. 6. (i) Transition in the antenna design. (ii) Change in antenna IV (Fig. 6(i)) with a bend in DRA and two feeding slots.

Table 3. Performance comparison of higher-order mode excited DRAs

Reference	Mode of excitation	Gain (dBi)	%BW
Petosa *et al.* (2009) [39]	$TE_{\delta 15}$	10.7	39.5
Pan *et al.* (2011) [49]	TE_{115}	5.8	13.47
	TE_{119}	6.3	
Hu *et al.* (2016) [47]	TE_{111}, TE_{311}, hybrid HEM	9.05	20.3
Pan *et al.* (2016) [48]	Higher	8.2	28.4
Ali *et al.* (2020) [43]	$TE^{x}_{\delta 15}$	10.5	16.1
Abdulmajid *et al.* (2020) [46]	TE_{511}, TE_{711}	9.45	35.8
Ji *et al.* (2022) [51]	Hybrid HEM and TMs	6.6	36.8

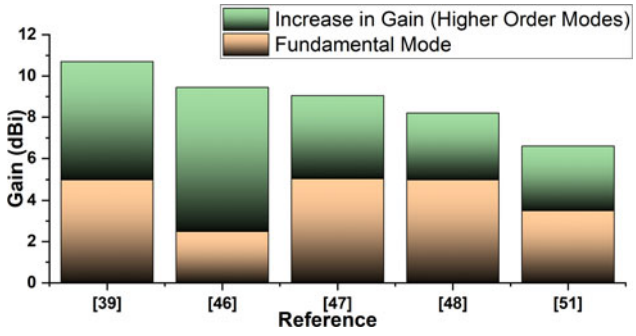

Fig. 7. Gain (dBi) increment using higher mode excitation.

mode and omnidirectional TM_{010} mode to operate in the same wide band, the center-loaded metal post also aids in improving resistance and significant matching of the TM_{010} resonance. Table 3 compares the performance of the antennas with higher-order mode excitation for enhanced gain. Figure 7 shows the graph indicating an increase in gain due to higher-order mode excitation. Though the higher-order mode excitation helps in improving circular polarization and percentage bandwidth, high power loss is reported in antennas which is a topic of concern. Frequency-selective surface (FSS) superstrates can be explored to overcome these limitations.

FSS superstrate

FSS are a growing research topic that provides spatially varying EM waves for selective frequency [52]. FSS merely exhibits an electrical response for a particular frequency [53–55]. FSS due to highly reflective surfaces increases the directivity considerably [56]. FSS [57–59] use metamaterials which are planar forms of meta-surfaces offering better and novel solutions as they shape the radiated wave by offering phase modulation which approaches 2π. According to Huygen's principle, exciting both electric and magnetic surface currents allows for unidirectional scattering providing maximum efficiency [60, 61]. Though FSS is not directly described as a gain enhancement technique, it eventually increases gain since gain (G) is related to directivity (D) and efficiency (η) by the relation given in equation (7).

$$G = D\eta \tag{7}$$

Kesavan *et al.* [62] suggested a DRA with FSS for mm-wave frequency band application. They proposed a cantilever-type four-layered FSS unit cell. The cantilevers are axe shaped with connecting lines cut out in stainless steel material which sits on the top layer and the bottom layer is a ground plane. Both layers are separated by epoxy resin glue. The CDRA acts as a radiating source and the FSS structure is placed on top of this CDRA separated by Rohacell foam. The DRA is excited using a coaxial probe. This FSS arrangement works as a parabolic reflector [63] increasing the gain up to 6 dBi. Figure 8 [62] explains this arrangement. Belen *et al.* [64] proposed a DRA loaded using FSS structure using 3D printing technology. The FSS inclusion provides moderate gain as well as reduces the antenna size considerably. Rana *et al.* [65] proposed a design with bandpass multilayer FSS to increase the gain of simple RDRA up to 3.6 dBi from normal RDRA design. Rana *et al.* [66] also proposed a dual-polarized RDRA with the same CRSF FSS superstrate. This antenna was found to be highly directive and dual polarization was applied using two microstrip lines exciting the DRA orthogonally. For an increase in gain, three split-ring resonators have been connected as a unit cell of an FSS which is polarization independent

https://doi.org/10.1017/S1759078723000119 Published online by Cambridge University Press

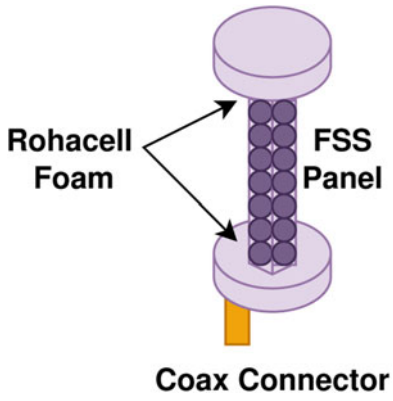

Fig. 8. Axe-shaped cantilever-based FSS structure.

providing a gain of 8.9 dBi. For the circularly polarized (CP) antenna, Akbari *et al.* [67] proposed and designed a wave frequency RDRA fed by coupling an *X*-shaped slot with one layer of FSS superstrate at the top to increase the gain to 8.5 dBi. Three layers of FSS provided a gain of 14.2 dBi. The increased gain is a result of a highly directive beam obtained in a broadside direction due to the reflected waves through the air gap being transmitted by the superstrate. The tuning of DRA, the air gap of the *X*-shaped slot, and the superstrate also play an important part in achieving the desired results. Such CP high-gain antennas can be effective in satellite communication applications. FSS are combined in MIMO antenna designs [68] at 60 GHz with low mutual coupling. For low mutual coupling in MIMO antennas, high isolation and low envelope correlation coefficient (ECC) are required [69]. ECC is related to diversity gain [69] as per equation (8). The FSS acts as a wall separation between two DRAs [68] to give high isolation. Also, the simulation gain is reported to increase by 1.5 dBi with respect to the reference antenna. In [70], Kakhki *et al.* reported a gain improvement of 4.2 dBi over the unloaded antenna by loading three layers of FSS horizontally in front of the ridge gap DRA in the *H*-plane. The resonant frequency of the antenna is 28 GHz and each layer of FSS consists of a 2×3 array of FSS unit cells. Chauhan *et al.* [71] reported a DRA for X-band applications with corrugated circular ring-shaped single-layer double-sided meta superstrate loaded on the DRA to enhance the peak gain to 11.9 dBi. A CDRA-based MIMO antenna is proposed by Das *et al.* [72] with multi-directional pattern diversity offering high isolation. The gain of this configuration is improved by 2.3 dBi which might be possible due to diverse radiation patterns in four directions as well as the low value of ECC. A coaxial RDRA for C-band applications [73] achieves a gain of 14 dBi by using an Metamaterial (MTM) superstrate of 50 cell units. The simple arrangement achieves a stable radiation pattern and circular polarization suitable for radar and satellite communication applications. In [74], the complementary split-ring resonators (CSRR) shaped slot is etched on HDRA and ground plane where current distribution which is out of phase lowers down. This results in current cancelation along the CSRR and hence reduces the cross-polar component of the radiation pattern thereby offering a gain of 6 dBi. Table 4 shows the performance comparison of FSS superstrate DRAs. Figure 9 shows the graph with an increase in gain using the FSS superstrate technique.

$$DG = 10\sqrt{1 - ECC^2} \tag{8}$$

Table 4. Performance comparison of FSS superstrate DRAs

Reference	Resonant frequency (GHz)	Gain (dBi)	% BW
Mukherjee *et al.* (2015) [74]	1.9	6	30
Rana *et al.* (2015) [65]	6.6	9.1	5
Rana *et al.* (2016) [66]	6.54	8.9	5.3
Akbari *et al.* (2016) [67]	30	15.5	8.26
Karimian *et al.* (2017) [68]	60	+1.5	10
Kesavan *et al.* (2018) [62]	30	8.1	–
Das *et al.* (2019) [72]	5.25	7.2	5
Pandey *et al.* (2019) [73]	7.8	14	16.1
Belen *et al.* (2020) [64]	2.4	5.6	29

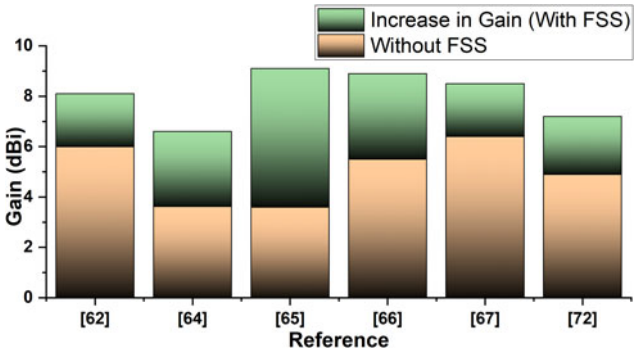

Fig. 9. Gain (dBi) increment using frequency-selective surfaces (FSS).

Electromagnetic band gap (EBG)

EBG is known to enhance the gain of the antenna by suppressing the unwanted surface wave [75–78]. It is experimentally proved by McKinzie *et al.* [78] that edge currents can be greatly reduced by EBG structure, and ground plane currents can be restricted. By restricting surface wave propagation, less diffraction occurs in non-broadside directions and broadside gain is increased. EBG has widely been used for beam tilting and enhancing the electrical properties of a DRA [79]. A reconfigurable radiation pattern in the azimuth plane was achieved in [79] by strategically placing six EBG sectors around the DRA. Circular-shaped EBG sectors were incorporated as they provide higher directivity as compared to other shapes [80, 81] and their performance is better in terms of EM wave suppression. This two-port EBG configured DRA [79] provides a gain of 4.2 dBi and is pattern reconfigurable as a pin diode is used for switching on and off the EBG sectors for the reconfigurability in azimuth plane at 60 GHz. The placement of EBG sectors around DRA is shown in Fig. 10 [79].

Mushroom-shaped EBG DRA for radar applications was proposed [82] and a comparison of non-EBG DRA and EBG DRA is presented. DRA with EBG improves the gain and a total gain of 6.7 dBi is achieved. Similarly, a 2.4 dBi improvement in gain was proposed [80] by placing the EBG structure 1 mm below the CDRA for mm-wave applications. Again, circular patch-based EBG [80, 81] was utilized and connected to the ground plane using vias. The design of DRA and EBG unit cells is optimized to lower the back radiation significantly [83] thereby blocking

https://doi.org/10.1017/S1759078723000119 Published online by Cambridge University Press

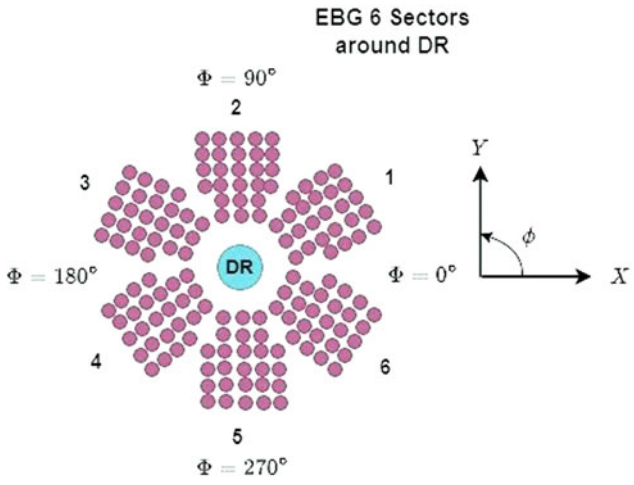

Fig. 10. Arrangement of six EBG sectors around DR.

the surface waves from propagating and hence increasing the radiation efficiency. Here, the EBG unit cells act as perfect magnetic conductors which cause impinging of surface waves propagating along the antenna substrates and diffracted at the edges thereby improving radiation efficiency and gain. Coulibaly *et al.* [84] suggested a new EBG substrate for CDRA for gain enhancement up to 3 dBi. Again, a circular-shaped EBG unit cell [80, 81] was utilized because in circular geometries located at the center of the source, the bandgap effect remains the same in all radial directions. So, the circular EBG was introduced on the substrate and connected to the ground plane through vias. Xia and Leung [85] reported a unique uniplanar EBG structure positioned around RDRA for gain enhancement of more than 3.5 dBi. The novelty of this design is that the EBG is placed around RDRA as shown in Fig. 11 which suppresses the surface wave, and its stopband features improve the radiation aperture of the antenna. The uniplanar design of the EBG unit cell consists of a patterned square patch in the center and four *L*-shaped patches at the corners for C-band applications. This feature of manipulation of the radiation patterns in antennas is explained in detail by Lee *et al.* [86]. They investigated the impediment in EM waves due to EBG materials for distinct types of antennas. Such structures enhance gain by suppressing the propagated wave at a particular frequency. In [87] EBG as a split-ring resonator structure is placed in the near field region of RDRA for gain enhancement. 5×5 array unit cell with a periodicity of $\lambda_0/6$ to $\lambda_0/8$ was placed above simple RDRA. The height of the superstrate is adjusted using parametric analysis which suppresses the RDRA as the first resonance of RDRA due to the loading effect and an increase in the number of unit cells increases the coupling and results in higher gain. This arrangement results in gain enhancement up to 1.5 dBi giving the final gain plot as 8 dBi. Gain enhancement techniques have gained much importance, especially for mm-wave as DRA's zero conductor loss feature makes it a suitable candidate for this frequency [88, 89]. Using a circular patch [80, 81] EBG for 60 GHz mm-wave frequencies gain enhancement was significantly achieved for DRAs [17, 90, 91]. In [17], a circular patch-based EBG structure is placed around CDRA like the one

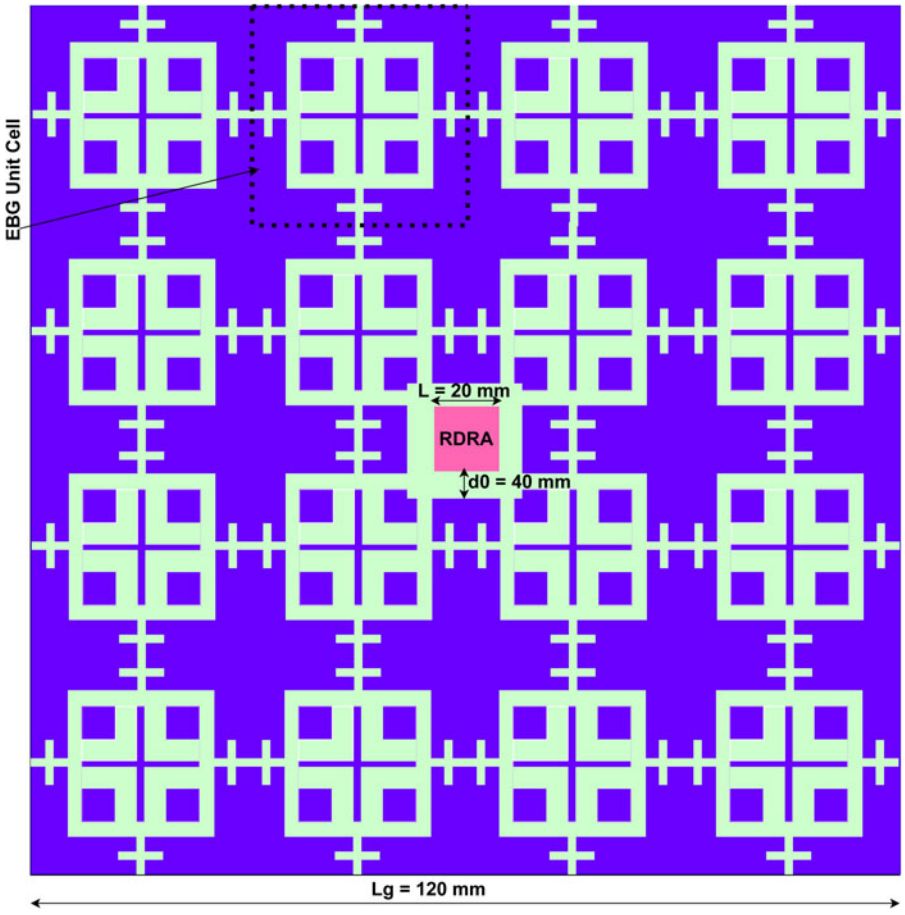

Fig. 11. RDRA with uniplanar EBG.

https://doi.org/10.1017/S1759078723000119 Published online by Cambridge University Press

presented in [85]. The distance between two EBG unit cells was calculated from equation (9) [92]:

$$\omega_{circular} = 1.1\ \omega_{square} - 0.1D \tag{9}$$

where ω is the gap width between two EBG unit cells and D is the period. No wave propagation is allowed in the frequency band and a large current induced in the circular patch lattice causes significant gain enhancement.

In [90], the EBG structure is used to feed the DRA and eliminate parasitic radiation from the feed line. A boresight gain of 12.6 dBi is reported. In [91], a printed ridge gap waveguide structure is used to feed the CDRA and acts as EBG to enhance the gain of CDRA. These techniques not only reduce the size of the antenna but also make DRA a successful antenna at mm-wave frequencies. A unique design is recently proposed in [93] where a compact and broad CP DRA using dielectric vias is designed. Filling a perforated printed circuit board (PCB) substrate with barium strontium titanate with a dielectric constant of 20 creates the dielectric vias. The electrical size of the DRA is lowered because of the highly effective dielectric constant of the dielectric vias-loaded PCB substrate. The DRA structure's layout of dielectric and air vias enables for spreading of the mode resonant frequencies of various radiating modes. This design incorporates a third higher-order mode into the passband, resulting in enhanced gain, impedance bandwidth, and axial ratio bandwidth. In [94] the EBG structure is introduced along the four side-wall boundaries of a particular dielectric region on a PCB to create a DR with fake EM boundaries. A printed array of periodic upside-down mushroom-type unit cells is used to create the EBG structure. The suggested DR can support both standard DR modes and dense dielectric patch cavity modes, according to the resonant-mode analysis. For developing a completely integrated DRA, a substrate-integrated gap waveguide transmission line is included in the proposed structure to excite the DR. Table 5 presents some of the comparative results of DRA using EBG structures and Fig. 12 shows the graph of the increase in gain using EBG structures. Even though EBG structures aid in increasing gain, they can be used with other methods to enhance the antenna's performance metrics. Hybrid antennas will be covered in the next part for better performance.

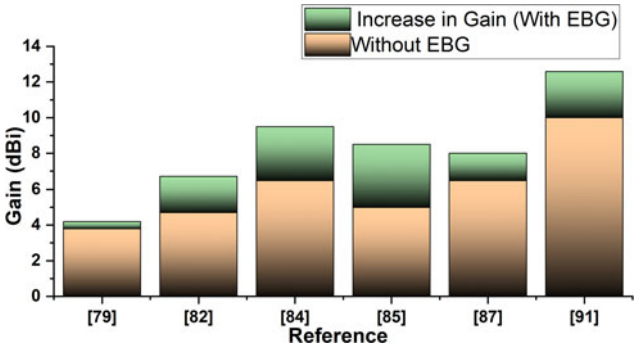

Fig. 12. Gain (dBi) increment using electromagnetic bandgap (EBG) structures.

Hybrid DRA

Another resort to increasing the gain of DRA is to incorporate the gain-enhancing properties of other antennas and form a hybrid antenna system. The disadvantage of such antennas can be the bulkier size. As seen in the stacked DRA section, Yagi–Uda designs were incorporated for increasing the gain [33]. However, this design increases fabrication complexities [95]. In [96–98], the DRAs are placed inside a horn for gain enhancement. In [96], RDRA is placed inside a short aluminum horn as was described in [97] for gain improvement and to make the antenna less bulky. Two microstrip lines are used for exciting the antenna [96] as well as stub loading is incorporated for bandwidth enhancement. The SMSH utilized here increases the directivity of the beam thereby increasing the boresight gain to 12.2 dBi. A very interesting and novel concept to increase the directivity and boresight gain to 11.3 dBi was proposed and investigated in [98] where a CDRA is placed inside a truncated conical horn made of plastic material. It is interesting to note that a non-conductive horn improves the gain by focusing the power in the boresight direction of the antenna. They also compared the solid conical horn with a notch-induced conical horn and found better results.

In [13], a copper-based hollow conical horn was placed around CDRA excited in its dominant HEM_{11} mode. In essence, the horn around DRA increases the directivity, and thereby increased gain

Table 5. Performance comparison of EBG superstrate DRAs

Reference	Resonant frequency (GHz)	Gain (dBi)	%BW	EBG unit cell shape
Coulibaly *et al.* (2007) [84]	2.25	+3	4.5	Circular
Mu'ath *et al.* (2012) [83]	60	+2.5	6.3	Mushroom
Abdelaal *et al.* (2016) [82]	9.5	6.7	31.5	Mushroom
Mu'ath *et al.* (2013) [17]	60	+3.2	11.6	Mushroom
Attia *et al.* (2017) [91]	62	9.5	20.5	Mushroom
Xia *et al.* (2018) [85]	3.5	9.4	9.3	Uniplanar
Sinha *et al.* (2018) [87]	4	8	41.4	Split-ring resonator
Al-Alem *et al.* (2019) [90]	60	12.6	27.5	Mushroom
Mabrouk *et al.* (2020) [79]	60	4.2	11.6	Circular
Tong *et al.* (2022) [93]	6.8	4.75	46.9	Vias
Ma *et al.* (2022) [94]	31	7.85	11.5	Mushroom

https://doi.org/10.1017/S1759078723000119 Published online by Cambridge University Press

is measured. Antennas as proposed in [99] provide circular polarization with a gain of around 2 dBi. High gain for millimeter waves in such antennas along with circular polarization could be challenging. In [100], an excellent gain of 16.71 dBi at 60 GHz is achieved using a cylindrical DR, a rectangular slot fed by a microstrip line, and stacked metallic strips [101, 102]. Metallic strips are placed at an optimized half wavelength height from the ground plane like FSS or EBG superstrates. Here it is important to note that the reflectivity is increased by selecting the optimized width of the microstrips as 0.7 mm. This causes the main lobe to be directed in a broadside direction. A different perspective of hybrid antennas was presented in [103] where a hollow is created in the DRA structure which is filled with water. The uneven structure of DRA consists of the lower layer as an irregular rectangular dielectric, an upper layer as a cylindrical dielectric with a center hollow part, a hybrid part of water, and a metal strip. The upper portion of DRA in the upper band has the most impact on the *E*-field distribution. The upper portion of DRA has a new structure because of the hybrid technology plan. Furthermore, this portion creates a high relative permittivity. The smaller cylindrical portion (water) forms the HEM_{111} mode at 2.75 GHz based only on the *E*-field properties of water. A new resonant mode is produced because of the interaction between the high order mode (TE_{113}) of the DRA and the mode of water. As a result, loading water activates the additional resonant mode at the upper band, which concentrates the energy of the upper section of DRA. The antenna's radiation performance in the *z*-axis direction is improved by the combination with high relative permittivity, which serves as a director and raises gain values from 6.01 to 8.33 dBic. Furthermore, by modifying the water volume, the gain values of HDRA at the upper band can be individually regulated as needed. Here, the water level is changed to achieve high gain operation, which has an impact on the combination part's relative permittivity. This increases gain in the upper band by 1.32 dB. In [104], a single chip-based array for terahertz frequency is investigated. A 2×2 array element with a single DRA placed on top of it increases the gain from 0.1 to 8.6 dBi at 340 GHz. Table 6 shows the performance comparison of some of the hybrid DRAs, and Fig. 13 provides a plot of the increase in gain using hybrid antennas.

DRA array

Gain enhancement can be achieved by cascading multiple antenna stages, for example, using antenna arrays. This not only scales up the overall size but also degrades the isolation. Isolation issues can be resolved using DRA arrays. An array of

Table 6. Performance comparison of hybrid DRAs

Reference	Resonant frequency (GHz)	Gain (dBi)	%BW
Esselle *et al.* (2007) [97]	6.5	9	21.3
Denidi *et al.* (2009) [13]	2.25	8.85	7
Agouzoul *et al.* (2011) [100]	60	16.7	12.6
Elboushi *et al.* (2014) [14]	30	11.2	3.8
Gupta *et al.* (2017) [96]	2.6	12.2	30
Baldazzi *et al.* (2020) [98]	30	11.3	16.6

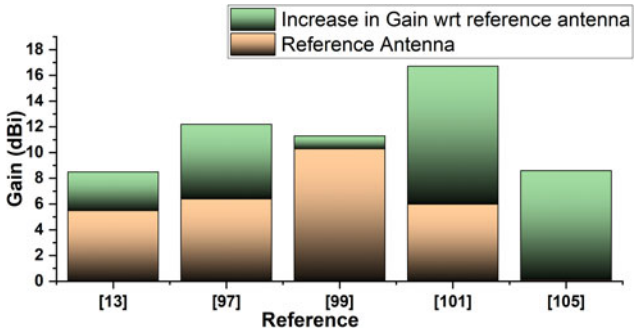

Fig. 13. Gain (dBi) increment using hybrid antenna structures.

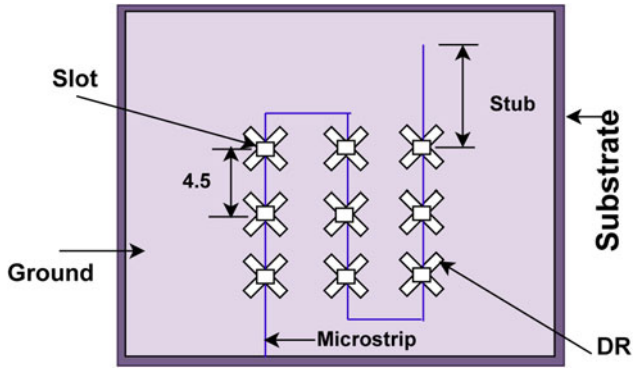

Fig. 14. Cross-shaped DRA array (AXDRA).

cross-shaped DRAs is presented in [105] which are excited using aperture coupling as shown in Fig. 14. A stub is introduced at the end of the microstrip line for better matching and this structure of nine-cross DRAs provides a gain of 15.5 dBi for mm-wave which is of great significance. A novel 4×10 array DRA structure was proposed and investigated for the frequency range of 90–110 GHz [106]. They incorporated a low-loss silicon image guide power splitter for feeding the array. This complex design [106] has overcome fabrication issues by incorporating the use of optical lithography and the silicon micromachining technique. The antenna theory concepts [107] are utilized in [108], and four-element triangular DRA is utilized to achieve a gain of 4.76 dBi. In [109], a bidirectional DRA array using a back-to-back quasi-Yagi antenna configuration is proposed where the DR is excited at higher-order mode increasing the gain by 1.8 dBi. Though this is an array configuration, it should be noted that higher-order mode excitation results in gain enhancement. In [110], Qureshi *et al.* suggested a cost-effective solution by creating cavities in acrylic templates and filling them with dielectric materials to build a polymer-based DRA array layer. This array-type antenna provides a gain of more than 10.5 dBi as reported by the authors. A similar approach of DRA array with a back cavity was reported in [111] with an enhanced gain of 17.2 dBi. In [112], without the use of power dividers, transitions, or launchers, a high-gain linear DRA array with a standing-wave feed network is proposed. In comparison to traditional feeding techniques, the suggested feed approach had a relatively high gain and outstanding efficiency. The manufacture of a four-element array using affordable 3D printing technology yielded a peak measured gain of 14 dBi. Table 7 shows the

https://doi.org/10.1017/S1759078723000119 Published online by Cambridge University Press

Table 7. Performance comparison of DRA arrays

Reference	Resonant frequency (GHz)	Gain (dBi)	%BW
Elkarkraoui *et al.* (2014) [105]	60	15.5	11
Zandeih *et al.* (2017) [106]	97	19	NA
Qureshi *et al.* (2017) [110]	60	10.5	12
Zhang *et al.* (2019) [104]	340	8.6	4.7
Chen *et al.* (2019) [111]	67	17.2	16.4
Ling-Ling Yang *et al.* (2020) [109]	10.34	7.58	7

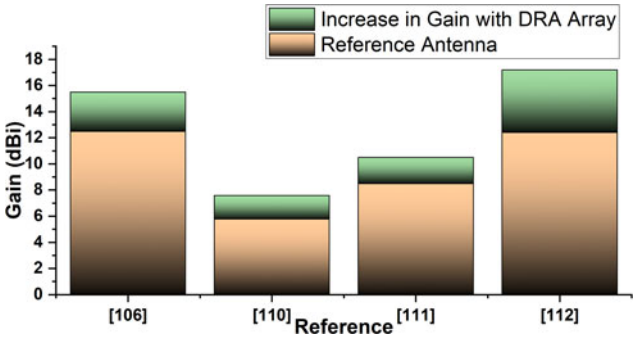

Fig. 15. Gain (dBi) increment using DRA arrays.

performance comparison of some of the DRA arrays and Fig. 15 provides a plot of the increase in gain using array antennas.

Comparison of gain enhancement techniques

Different techniques to enhance gain have been presented in section "Gain enhancement techniques". It can be deduced from the study that an array of DRA with moderate gain can be used for adequate area coverage as mentioned by Baldazzi *et al.* [98] and Varshney *et al.* [99]. For miniaturized applications, FSS and EBG structures can be incorporated for gain enhancement. Radiation pattern significantly improves with the help of hybrid DRAs increasing the gain. Stacking is the simplest technique that not only improves gain but also bandwidth but is bulkier and costly. A detailed comparison of each technique is presented in tabular form for better vision and understanding. Table 8 presents the range of gain and percentage bandwidth obtained from each technique as discussed.

Conclusions and future scope

In this paper, we present a comprehensive comparison of different gain enhancement techniques in DRAs. Various techniques for stacked DRA and higher-order mode excitation are found to achieve higher gains up to 10 dBi. However, the stacking of DRA makes it more costly and bulky, thereby suited for very limited applications. The higher-order mode excitation increases the power losses, making it unsuitable for mm-wave frequencies. For mm-wave and higher frequencies FSS and EBG, superstrate/structures are utilized. However, the complexities of these structures and the excitation of surface waves that leads to lower bandwidth

Table 8. Comparison of gain enhancement techniques

Technique	Range of gain obtained (dBi)	Range of % bandwidth obtained	Possible applications
Stacking	6–10.5	2.7–63.2	UWB applications
Higher-order modes	5–10.5	13.47–97.4	5G, wireless communication
FSS	5.6–15.5	5–30	5G MIMO
EBG	4.2–12.6	4.5–46.9	Spatial filters, 5G
Hybrid DRA	9–16.7	3.8–21.3	Satellite communication, radar
DRA Array	8.6–15.5	3–21	MIMO

cannot be denied. FSS can provide a gain enhancement of up to 15.5 dBi [67] whereas EBG structures can achieve a gain enhancement of up to 12.6 dBi [90]. To maintain the performance parameters, hybrid antennas can be deployed to achieve a gain enhancement of up to 16.7 dBi [100]. Hybrid antennas being bulkier open the scope for space-constrained research. If the size is not a priority, the DRA array techniques can be explored in MIMO applications for gain enhancement and to provide the desired performance parameters. A gain of up to 19 dBi [106] has been reported for DRA arrays. We have focused on the mm-wave frequency band in the later part, as it is still an unexplored frequency range and is a future for the 5G wireless communication domain. Despite several advantages, DRAs also have certain limitations including the physical characteristics of the material, their fabrication, and their placement restriction on the PCB. To address this, DRAs are also being explored at the nanometer level [112] that are suitable for wireless communication. The frequency range can be improved by using DRA arrays along with ease of fabrication and manufacturing techniques. Miniaturization and ease of manufacturing make DRAs practically viable and useful for massive MIMO [113, 114]. Moreover, the utilization of a single mask for fabrication and combining the Complementary Metal Oxide Semiconductor(CMOS) technology in DRA fabrication [115] can be useful in the development of DRA structures.

Acknowledgements. The survey could not be completed without valuable inputs from Dr. Paritosh Peshwe, Assistant Professor, Indian Institute of Information Technology, Nagpur, India. We would also like to thank the reviewers for their useful comments and suggestions. This paper is a part of the fellowship of the Visvesveraya Ph.D. scheme (part-time), MIETY, Government of India.

Conflict of interest. None.

References

1. **Keyrouz S and Caratelli D** (2016) Dielectric resonator antennas: basic concepts, design guidelines, and recent developments at millimeter-wave frequencies. *International Journal of Antennas and Propagation* **2016**, 1–20.
2. **McAllister MW, Andrew Long S and Conway GL** (1983) Rectangular dielectric resonator antenna. *Electronics Letters* **19**, 218.
3. **McAllister MW and Andrew Long S** (1984) Resonant hemispherical dielectric antenna. *Electronics Letters* **20**, 657–659.

https://doi.org/10.1017/S1759078723000119 Published online by Cambridge University Press

4. **Kranenburg RA and Long SA** (1988) Microstrip transmission line excitation of dielectric resonator antennas. *Electronics Letters* **24**, 1156.
5. **Petosa A, Simons N, Siushansian R, Ittipiboon A and Cuhaci M** (2000) Design and analysis of multisegment dielectric resonator antennas. *IEEE Transactions on Antennas and Propagation* **48**, 738–742.
6. **Leung KW, Lim EH and Fang XS** (2012) Dielectric resonator antennas: from the basic to the aesthetic. *Proceedings of the IEEE* **100**, 2181–2193.
7. **Gupta A and Gangwar RK** (2019) Hybrid rectangular dielectric resonator antenna for multiband applications. *IETE Technical Review* **37**, 83–90.
8. **Nor NM, Jamaluddin MH, Kamarudin MR and Khalily M** (2016) Rectangular dielectric resonator antenna array for 28 GHz applications. *Progress in Electromagnetics Research* **63**, 53–61.
9. **Wang Y, Denidni T, Zeng Q and Wei G** (2013) A wideband high-gain stacked cylindrical dielectric resonator antenna. *Progress in Electromagnetics Research Letters* **43**, 155–163.
10. **Coulibaly Y, Nedil M, Talbi L and Denidni TA** (2010) High gain cylindrical dielectric resonator with superstrate for broadband millimeter-wave underground mining communications. In *2010 14th International Symposium on Antenna Technology and Applied Electromagnetics & the American Electromagnetics Conference (pp. 1–4)*. IEEE.
11. **Feng W, Li Y, Jin D, Su L and Chen S** (2016) Millimetre-wave backhaul for 5G networks: challenges and solutions. *Sensors* **16**, 892.
12. **Rappaport TS, Xing Y, MacCartney GR, Molisch AF, Mellios E and Zhang J** (2017) Overview of millimeter wave communications for fifth-generation (5G) wireless networks-with a focus on propagation models. *IEEE Transactions on Antennas and Propagation* **65**, 6213–6230.
13. **Denidni TA, Coulibaly Y and Boutayeb H** (2009) Hybrid dielectric resonator antenna with circular mushroom-like structure for gain improvement. *IEEE Transactions on Antennas and Propagation* **57**, 1043–1049.
14. **Elboushi A and Sebak AR** (2014) High gain hybrid DRA/horn antenna for MMW applications. In *2014 IEEE Antennas and Propagation Society International Symposium (APSURSI) (pp. 1968–1969)*. IEEE.
15. **Guha D, Banerjee A, Kumar C and Antar YM** (2011) Higher order mode excitation for high-gain broadside radiation from cylindrical dielectric resonator antennas. *IEEE Transactions on Antennas and Propagation* **60**, 71–77.
16. **Perron A, Denidni TA and Sebak AR** (2009) High-gain hybrid dielectric resonator antenna for millimeter-wave applications: design and implementation. *IEEE Transactions on Antennas and Propagation* **57**, 2882–2892.
17. **Mu'ath J, Denidni TA and Sebak AR** (2013) Millimeter-wave EBG-based aperture-coupled dielectric resonator antenna. *IEEE Transactions on Antennas and Propagation* **61**, 4354–4357.
18. **Lai Q, Fumeaux C, Hong W and Vahldieck R** (2010) 60 GHz aperture-coupled dielectric resonator antennas fed by a half-mode substrate integrated waveguide. *IEEE Transactions on Antennas and Propagation* **58**, 1856–1864.
19. **Guha D and Kumar C** (2016) Microstrip patch versus dielectric resonator antenna bearing all commonly used feeds: an experimental study to choose the right element. *IEEE Antennas and Propagation Magazine* **58**, 45–55.
20. **Cicchetti R, Faraone A, Miozzi E, Ravanelli R and Testa O** (2016) A high-gain mushroom-shaped dielectric resonator antenna for wideband wireless applications. *IEEE Transactions on Antennas and Propagation* **64**, 2848–2861.
21. **Fakhte S, Oraizi H and Matekovits L** (2016) High gain rectangular dielectric resonator antenna using uniaxial material at fundamental mode. *IEEE Transactions on Antennas and Propagation* **65**, 342–347.
22. **Petosa A and Thirakoune S** (2011) Rectangular dielectric resonator antennas with enhanced gain. *IEEE Transactions on Antennas and Propagation* **59**, 1385–1389.
23. **Pan YM and Zheng SY** (2015) A low-profile stacked dielectric resonator antenna with high-gain and wide bandwidth. *IEEE Antennas and Wireless Propagation Letters* **15**, 68–71.
24. **Esselle KP** (1996) A low-profile rectangular dielectric-resonator antenna. *IEEE Transactions on Antennas and Propagation* **44**, 1296–1297.
25. **Mongia RK** (1994) Low profile dielectric resonator antennas using a very high permittivity material. *Electronics Letters* **30**, 1362–1363.
26. **Hwang Y, Zhang YP, Luk KM and Yung EK** (1997) Gain-enhanced miniaturized rectangular dielectric resonator antenna. *Electronics Letters* **33**, 350–352.
27. **Yarga S, Sertel K and Volakis JL** (2009) Multilayer dielectric resonator antenna operating at degenerate band edge modes. *IEEE Antennas and Wireless Propagation Letters* **8**, 287–290.
28. **Yarga S, Sertel K and Volakis JL** (2009) A directive resonator antenna using degenerate band edge crystals. *IEEE Transactions on Antennas and Propagation* **57**, 799–803.
29. **Lee JK and Kong JA** (1983) Dyadic Green's functions for layered anisotropic medium. *Electromagnetics* **3**, 111–130.
30. **Eroglu A and Lee JK** (2005) Far field radiation from an arbitrarily oriented Hertzian dipole in the presence of a layered anisotropic medium. *IEEE Transactions on Antennas and Propagation* **53**, 3963–3973.
31. **Pettis GF** (2008) *Hertzian Dipoles and Microstrip Circuits on Arbitrarily Oriented Biaxially Anisotropic Media*. New York: Syracuse University.
32. **Fakhte S and Oraizi H** (2016) Analysis and design of rectangular uniaxial and biaxial anisotropic dielectric resonator antennas. *Progress in Electromagnetics Research C* **62**, 43–50.
33. **Kishk AA** (2005) Directive Yagi–Uda dielectric resonator antennas. *Microwave and Optical Technology Letters* **44**, 451–453.
34. **Xia ZX and Leung KW** (2022) 3-D-printed wideband circularly polarized dielectric resonator antenna with two printing materials. *IEEE Transactions on Antennas and Propagation* **70**, 5971–5976.
35. **Bit-Babik G, Di Nallo C and Faraone A** (2004) Multimode dielectric resonator antenna of very high permittivity. In *IEEE Antennas and Propagation Society Symposium, 2004. (Vol. 2, pp. 1383–1386)*. IEEE.
36. **Li B and Leung KW** (2005) A wideband strip-fed rectangular dielectric resonator antenna. In *2005 IEEE Antennas and Propagation Society International Symposium (Vol. 2, pp. 172–175)*. IEEE.
37. **De Young CS and Long SA** (2006) Wideband cylindrical and rectangular dielectric resonator antennas. *IEEE Antennas and Wireless Propagation Letters* **5**, 426–429.
38. **Hwang Y, Zhang YP, Zheng GX and Lo TK** (1995) Planar inverted F antenna loaded with high permittivity material. *Electronics Letters* **31**, 1710–1712.
39. **Petosa A, Thirakoune S and Ittipiboon A** (2009) Higher-order modes in rectangular DRAs for gain enhancement. In *2009 13th International Symposium on Antenna Technology and Applied Electromagnetics and the Canadian Radio Science Meeting (pp. 1–4)*. IEEE.
40. **Mongia RK and Bhartia P** (1994) Dielectric resonator antennas – a review and general design relations for resonant frequency and bandwidth. *International Journal of Microwave and Millimeter-Wave Computer-Aided Engineering* **4**, 230–247.
41. **Mongia RK and Ittipiboon A** (1997) Theoretical and experimental investigations on rectangular dielectric resonator antennas. *IEEE Transactions on Antennas and Propagation* **45**, 1348–1356.
42. **Khan QU, Ihsan MB, Fazal D, Malik FM, Sheikh SA and Salman M** (2016) Higher order modes: a solution for high gain, wide band patch antennas for different vehicular applications. *IEEE Transactions on Vehicular Technology* **66**, 3548–3554.
43. **Ali I, Jamaluddin MH, Gaya A and Rahim HA** (2020) A dielectric resonator antenna with enhanced gain and bandwidth for 5G applications. *Sensors* **20**, 675.
44. **Liang XL and Denidni TA** (2008) H-shaped dielectric resonator antenna for wideband applications. *IEEE Antennas and Wireless Propagation Letters* **7**, 163–166.
45. **Fakhte S, Oraizi H and Matekovits L** (2017) Gain improvement of rectangular dielectric resonator antenna by engraving grooves on its side walls. *IEEE Antennas and Wireless Propagation Letters* **16**, 2167–2170.

https://doi.org/10.1017/S1759078723000119 Published online by Cambridge University Press

46. **Abdulmajid AA, Khamas S and Zhang S** (2020) Wideband high-gain millimetre-wave three-layer hemispherical dielectric resonator antenna. *Progress in Electromagnetics Research C* **103**, 225–236.
47. **Hu PF, Pan YM, Zhang XY and Zheng SY** (2016) A compact filtering dielectric resonator antenna with wide bandwidth and high gain. *IEEE Transactions on Antennas and Propagation* **64**, 3645–3651.
48. **Pan YM, Hu PF, Zhang XY and Zheng SY** (2016) A low-profile high-gain and wideband filtering antenna with metasurface. *IEEE Transactions on Antennas and Propagation* **64**, 2010–2016.
49. **Pan YM, Leung KW and Luk KM** (2011) Design of the millimeter-wave rectangular dielectric resonator antenna using a higher-order mode. *IEEE Transactions on Antennas and Propagation* **59**, 2780–2788.
50. **Koul SK** (1997) *Millimeter Wave Optical Dielectric Integrated Guides and Circuits*. New York: Wiley-Interscience.
51. **Ji Y, Ge L, Li Y and Wang J** (2022) Wideband polarization agile dielectric resonator antenna with reconfigurable broadside and conical beams. *IEEE Transactions on Antennas and Propagation* **70**, 7169–7174.
52. **Anwar RS, Mao L and Ning H** (2018) Frequency selective surfaces: a review. *Applied Sciences* **8**, 1689.
53. **Glybovski SB, Tretyakov SA, Belov PA, Kivshar YS and Simovski CR** (2016) Metasurfaces: from microwaves to visible. *Physics Reports* **634**, 1–72.
54. **Munk BA** (2000) *Frequency Selective Surfaces: Theory and Design*, Vol. **29**. Hoboken, NJ, USA: Wiley Online Library.
55. **Vardaxoglou JC** (1997) *Frequency Selective Surfaces: Analysis and Design*. Boston, MA, USA: Research Studies Press.
56. **Munk BA** (2005) *Frequency Selective Surfaces: Theory and Design*. New York: John Wiley & Sons.
57. **Kapoor A, Mishra R and Kumar P** (2022) Frequency selective surfaces as spatial filters: fundamentals, analysis and applications. *Alexandria Engineering Journal* **61**, 4263–4293.
58. **Celozzi S, Araneo R, Burghignoli P and Lovat G** (2023) Frequency selective surfaces, in Electromagnetic Shielding: Theory and Applications, IEEE, 2023, pp. 363–408, doi: 10.1002/9781119736318.ch12.
59. **Lalbakhsh A, Afzal MU, Esselle KP and Smith SL** (2022) All-metal wideband frequency-selective surface bandpass filter for TE and TM polarizations. *IEEE Transactions on Antennas and Propagation* **70**, 2790–2800.
60. **Pfeiffer C and Grbic A** (2013) Metamaterial Huygens' surfaces: tailoring wave fronts with reflectionless sheets. *Physical Review Letters* **110**, 197401.
61. **Tsilipakos O, Koschny T and Soukoulis CM** (2018) Antimatched electromagnetic metasurfaces for broadband arbitrary phase manipulation in reflection. *ACS Photonics* **5**, 1101–1107.
62. **Kesavan A, Mantash M, Zaid J and Denidni TA** (2018) A dual-plane beam-sweeping millimeter-wave antenna using reconfigurable frequency selective surfaces. *IEEE Antennas and Wireless Propagation Letters* **17**, 1832–1836.
63. **Niroo-Jazi M and Denidni TA** (2012) Electronically sweeping-beam antenna using a new cylindrical frequency-selective surface. *IEEE Transactions on Antennas and Propagation* **61**, 666–676.
64. **Belen MA, Mahouti P and Palandöken M** (2020) Design and realization of novel frequency selective surface loaded dielectric resonator antenna via 3D printing technology. *Microwave and Optical Technology Letters* **62**, 2004–2013.
65. **Rana B, Chatterjee A and Parui SK** (2015) Gain enhancement of a direct microstrip line fed dielectric resonator antenna using FSS. In *2015 IEEE Applied Electromagnetics Conference (AEMC) 2015 Dec 18 (pp. 1–2)*. IEEE.
66. **Rana B, Chatterjee A and Parui SK** (2016) Gain enhancement of a dual-polarized dielectric resonator antenna using polarization independent FSS. *Microwave and Optical Technology Letters* **58**, 1415–1420.
67. **Akbari M, Gupta S, Farahani M, Sebak AR and Denidni TA** (2016) Gain enhancement of circularly polarized dielectric resonator antenna based on FSS superstrate for MMW applications. *IEEE Transactions on Antennas and Propagation* **64**, 5542–5546.
68. **Karimian R, Kesavan A, Nedil M and Denidni TA** (2016) Low-mutual-coupling 60-GHz MIMO antenna system with frequency selective surface wall. *IEEE Antennas and Wireless Propagation Letters* **16**, 373–376.
69. **Costa JR, Lima EB, Medeiros CR and Fernandes CA** (2011) Evaluation of a new wideband slot array for MIMO performance enhancement in indoor WLANs. *IEEE Transactions on Antennas and Propagation* **59**, 1200–1206.
70. **Kakhki MB, Mousavirazi Z and Denidni TA** (2019) High gain ridge gap dielectric resonator antenna using FSS superstrates. In *2019 IEEE International Symposium on Antennas and Propagation and USNC-URSI Radio Science Meeting 2019 Jul 7 (pp. 71–72)*. IEEE.
71. **Chauhan M, Rajput A and Mukherjee B** (2021) Wideband circularly polarized low profile dielectric resonator antenna with meta superstrate for high gain. *AEU-International Journal of Electronics and Communications* **128**, 153524.
72. **Das G, Sahu NK, Sharma A, Gangwar RK and Sharawi MS** (2019) FSS-based spatially decoupled back-to-back four-port MIMO DRA with multidirectional pattern diversity. *IEEE Antennas and Wireless Propagation Letters* **18**, 1552–1556.
73. **Pandey AK, Chauhan M, Killamsety VK and Mukherjee B** (2019) High-gain compact rectangular dielectric resonator antenna using metamaterial as superstrate. *International Journal of RF and Microwave Computer-Aided Engineering* **29**, e21968.
74. **Mukherjee B, Patel P and Mukherjee J** (2015) A novel hemispherical dielectric resonator antenna with complementary split-ring-shaped slots and resonator for wideband and low cross-polar applications. *IEEE Antennas and Propagation Magazine* **57**, 120–128.
75. **Adas E, De Flaviis F and Alexopoulos NG** (2018) Realization of scan blindness free finite microstrip phased arrays based on mode-free radiating electromagnetic bandgap materials. *IEEE Transactions on Antennas and Propagation* **66**, 3375–3382.
76. **Mourtzios C and Siakavara K** (2017) Contribution of non-uniform EBG antenna arrays to the enhancement of MIMO channel capacity. *AEU-International Journal of Electronics and Communications* **82**, 334–340.
77. **Wang M and Chu QX** (2019) A wideband polarization-reconfigurable water dielectric resonator antenna. *IEEE Antennas and Wireless Propagation Letters* **18**, 402–406.
78. **McKinzie WE, Nair DM, Thrasher BA, Smith MA, Hughes ED and Parisi JM** (2016) 60-GHz 2×2 LTCC patch antenna array with an integrated EBG structure for gain enhancement. *IEEE Antennas and Wireless Propagation Letters* **15**, 1522–1525.
79. **Mabrouk IB, Nedil M, Denidni TA and Sebak AR** (2019) A novel design of radiation pattern-reconfigurable antenna system for millimeter-wave 5G applications. *IEEE Transactions on Antennas and Propagation* **68**, 2585–2592.
80. **Al-Hassan MAJ** (2015) *Millimeter-wave Electromagnetic Band-gap Structures for Antenna and Antenna Arrays Applications* (Doctoral dissertation), Quebec and Canada: Université du Québec, Institut national de la recherche scientifique.
81. **Mabrouk IB, E'qab RF, Nedil M and Denidni TA** (2019) Hybrid isolator for mutual-coupling reduction in millimeter-wave MIMO antenna systems. *IEEE Access* **7**, 58466–58474.
82. **Abdelaal MA and Kishk AA** (2016) Dielectric resonator antenna gain improvement using electromagnetic band gap surface for radar applications. In *2016 17th International Symposium on Antenna Technology and Applied Electromagnetics (ANTEM) 2016 Jul 10 (pp. 1–2)*. IEEE.
83. **Mu'ath J, Denidni TA and Sebak AR** (2012) EBG dielectric-resonator antenna with reduced back radiation for millimeter-wave applications. In *Proceedings of the 2012 IEEE International Symposium on Antennas and Propagation 2012 Jul 8 (pp. 1–2)*. IEEE.
84. **Coulibaly Y, Boutayeb H, Denidni TA and Talbi L** (2007) Gain enhancement of a dielectric resonator antenna using a cylindrical

https://doi.org/10.1017/S1759078723000119 Published online by Cambridge University Press

electromagnetic crystal substrate. In *2007 IEEE Antennas and Propagation Society International Symposium 2007 Jun 9 (pp. 1325–1328)*. IEEE.
85. **Xia ZX and Leung KW** (2018) Gain enhancement of rectangular dielectric resonator antenna using EBG surface. In *2018 IEEE Asia-Pacific Conference on Antennas and Propagation (APCAP) 2018 Aug 5 (pp. 102–103)*. IEEE.
86. **Lee Y, Yeo J and Mittra R** (1999) Investigation of electromagnetic bandgap (EBG) structures for antenna pattern control. In *IEEE Antennas and Propagation Society International Symposium 2003 Jun 22 (Vol. 2, pp. 1115–1118)*. IEEE.
87. **Sinha M, Killamsetty V and Mukherjee B** (2018) Near field analysis of RDRA loaded with split ring resonators superstrate. *Microwave and Optical Technology Letters* **60**, 472–478.
88. **Long S, McAllister M and Shen L** (1983) The resonant cylindrical dielectric cavity antenna. *IEEE Transactions on Antennas and Propagation* **31**, 406–412.
89. **Jazi MN and Denidni TA** (2008) Design and implementation of an ultrawideband hybrid skirt monopole dielectric resonator antenna. *IEEE Antennas and Wireless Propagation Letters* **7**, 493–496.
90. **Al-Alem Y and Kishk AA** (2019) Wideband millimeter-wave dielectric resonator antenna with gain enhancement. *IEEE Antennas and Wireless Propagation Letters* **18**, 2711–2715.
91. **Attia H and Kishk AA** (2017) Wideband self-sustained DRA fed by printed ridge gap waveguide at 60 GHz. In *2017 IEEE 28th Annual International Symposium on Personal, Indoor, and Mobile Radio Communications (PIMRC) 2017 Oct 8 (pp. 1–3)*. IEEE.
92. **Ramaccia D, Toscano A and Bilotti F** (2011) A new accurate model of high-impedance surfaces consisting of circular patches. *Progress in Electromagnetics Research M* **21**, 1–7.
93. **Tong C, Hauke KI, Yang N and Leung KW** (2022) Compact wideband circularly polarized dielectric resonator antenna with dielectric vias. *IEEE Antennas and Wireless Propagation Letters* **21,** 1100–1104.
94. **Ma C, Zheng SY, Pan YM and Chen Z** (2022) Millimeter-wave fully integrated dielectric resonator antenna and its multi-beam application. *IEEE Transactions on Antennas and Propagation* **70**, 6571–6580.
95. **Kramer O, Djerafi T and Wu K** (2011) Very small footprint 60 GHz stacked Yagi antenna array. *IEEE Transactions on Antennas and Propagation* **59**, 3204–3210.
96. **Gupta RD and Parihar MS** (2017) Differentially fed wideband rectangular DRA with high gain using short horn. *IEEE Antennas and Wireless Propagation Letters* **16**, 1804–1807.
97. **Esselle KP** (2007) A low-profile compact microwave antenna with high gain and wide bandwidth. *IEEE Transactions on Antennas and Propagation* **55**, 1880–1883.
98. **Baldazzi E, Al-Rawi A, Cicchetti R, Smolders AB, Testa O, van Coevorden Moreno CD and Caratelli D** (2020) A high-gain dielectric resonator antenna with plastic-based conical horn for millimeter-wave applications. *IEEE Antennas and Wireless Propagation Letters* **19**, 949–953.
99. **Varshney G, Pandey VS and Yaduvanshi RS** (2018) Axial ratio bandwidth enhancement of a circularly polarized rectangular dielectric resonator antenna. *International Journal of Microwave and Wireless Technologies* **10**, 984–990.
100. **Agouzoul A, Nedil M, Coulibaly Y, Denidni TA, Mabrouk IB and Talbi L** (2011) Design of a high gain hybrid dielectric resonator antenna for millimeter-waves underground applications. In *2011 IEEE International Symposium on Antennas and Propagation (APSURSI) 2011 Jul 3 (pp. 1688–1691)*. IEEE.
101. **Moustafa L and Jecko B** (2010) Design of a wideband highly directive EBG antenna using double-layer frequency selective surfaces and multi-feed technique for application in the Ku-band. *IEEE Antennas and Wireless Propagation Letters* **9**, 342–346.
102. **Rodes E, Diblanc M, Arnaud E, Monediere T and Jecko B** (2007) Dual-band EBG resonator antenna using a single-layer FSS. *IEEE Antennas and Wireless Propagation Letters* **6**, 368–371.
103. **Lin KZ and Wu TT** (2022) Dual-band circularly polarized hybrid dielectric resonator antenna with gain enhancement. *AEU-International Journal of Electronics and Communications* **146**, 154121.
104. **Zhang Y, Deng JY, Li MJ, Sun D and Guo LX** (2019) A MIMO dielectric resonator antenna with improved isolation for 5G mm-wave applications. *IEEE Antennas and Wireless Propagation Letters* **18**, 747–751.
105. **Elkarkraoui T, Delisle GY, Hakem N and Coulibaly Y** (2014) High gain cross DRA antenna array for underground communications. In *2014 IEEE Antennas and Propagation Society International Symposium (APSURSI) 2014 Jul 6 (pp. 1942–1943)*. IEEE.
106. **Zandieh A, Abdellatif AS, Taeb A and Safavi-Naeini S** (2017) High resistivity silicon DRA array for millimeter-wave high gain applications. In *2017 IEEE MTT-S International Microwave Symposium (IMS) 2017 Jun 4 (pp. 857–860)*. IEEE.
107. **Mukherjee B, Patel P and Mukherjee J** (2020) A review of the recent advances in dielectric resonator antennas. *Journal of Electromagnetic Waves and Applications* **34**, 1095–1158.
108. **Gangwar RK, Ranjan P and Aigal A** (2017) Four element triangular dielectric resonator antenna for wireless application. *International Journal of Microwave and Wireless Technologies* **9**, 113–119.
109. **Yang LL, Ke YH and Chen JX** (2020) An X-band gain-enhanced bidirectional antenna array using strip-loaded dielectric resonator operating in TE3δ1 mode. *International Journal of Microwave and Wireless Technologies* **12**, 915–921.
110. **Qureshi AA, Klymyshyn DM, Tayfeh M, Mazhar W, Börner M and Mohr J** (2017) Template-based dielectric resonator antenna arrays for millimeter-wave applications. *IEEE Transactions on Antennas and Propagation* **65**, 4576–4584.
111. **Chen Z, Shen C, Liu H, Ye X, Qi L, Yao Y, Yu J and Chen X** (2019) Millimeter-wave rectangular dielectric resonator antenna array with enlarged DRA dimensions, wideband capability, and high-gain performance. *IEEE Transactions on Antennas and Propagation* **68**, 3271–3276.
112. **Abdalmalak KA, Althuwayb AA, Lee CS, Botello GS, Falcón-Gómez E, García-Castillo LE and García-Muñoz LE** (2022) Standing-wave feeding for high-gain linear dielectric resonator antenna (DRA) array. *Sensors* **22**, 3089.
113. **Varshney G and Sahana BC** (2022) Implementing the single/multiport tunable terahertz circularly polarized dielectric resonator antenna. *Nano Communication Networks* **32**, 100408.
114. **Malekar RR, Raut H, Shevada L and Kumar S** (2021) A review on MIMO dielectric resonator antenna for 5G application. *Micro-Electronics and Telecommunication Engineering: Proceedings of 4th ICMETE 2020. 2021 May 29*, pp. 1–8.
115. **Hou D, Hong W, Goh WL, Chen J, Xiong YZ, Hu S and Madihian M** (2014) D-band on-chip higher-order-mode dielectric-resonator antennas fed by half-mode cavity in CMOS technology. *IEEE Antennas and Propagation Magazine* **56**, 80–89.

Ankita H. Harkare pursued her Bachelor of Engineering (electronics and communication) and Masters in Engineering (VLSI design) from Shri Ramdeobaba College of Engineering and Management, Nagpur, India in 2009 and 2014, respectively. She is currently pursuing her Ph.D. from the Indian Institute of Information Technology, Nagpur, India. She worked as a system engineer at Tata Consultancy Services after completion of graduation. She is currently working as an assistant professor at Shri Ramdeobaba College of Engineering and Management, Nagpur, India. She has attended and presented papers at eight national and international conferences and published 11 journal papers to date. She has three published patents, three copyright, and one book chapter in Springer Series to her credit. She has delivered expert lectures in the field of VLSI design and conducted workshops related to the same. Her current research interest is antenna design. She is a life member of ISTE and IAENG.

https://doi.org/10.1017/S1759078723000119 Published online by Cambridge University Press

Dr. Ashwin G. Kothari is currently working as an associate professor in the Electronics and Communication Engineering Department of Visvesvaraya National Institute of Technology, Nagpur, India from where he has received his Ph.D. in 2010. He is also one of the coordinators for the Center of Excellence of Commbedded Systems: Hybridization of Communications and Embedded Systems established as a World Bank-assisted project of TEQIP 1.2.1. Applications of rough set-based signal processing are his special interest. He has authored several publications and has contributed book chapters for reputed publications. He has 25+ years of experience in teaching and research. He has produced eight Ph.D.s so far and is still guiding five Ph.D.s under his supervision. He has been a resource person for many seminars, invited talks, workshops, etc. He has eight filed patents and worked on industry collaborative projects with industries like Tektronix, Mathworks, NI, HCIT, SAMEER Mumbai, etc.

Ankit A. Bhurane is currently working as an assistant professor in the Department of Electronics and Communication, Indian Institute of Information Technology Nagpur. He received his B.E. in electronics and communication, M.Tech. in electronics, and Ph.D. in 2008, 2011, and 2016, respectively, from SGBAU University, SGGS Nanded, and IIT Bombay. He has published papers in various international conferences and journals. He also has published a patent registered in the Indian Patent Office. His research interests include biomedical signal processing, scalable video coding, and green communication.

https://doi.org/10.1017/S1759078723000119 Published online by Cambridge University Press